Computers and Electronics in Agriculture 127 (2016) 289–301

Contents lists available at ScienceDirect

Computers and Electronics in Agriculture

journal homepage: www.elsevier.com/locate/compag

Original papers

Remote detection of light tolerance in Basil through frequency and transient analysis of light induced fluorescence

Anna-Maria Carstensen [a,*], Tessa Pocock [b], Daniel Bånkestad [c], Torsten Wik [a]

[a] Chalmers University of Technology, Gothenburg, Sweden
[b] Smart Lighting Engineering Research Center, Rensselaer Polytechnic Institute, Troy, NY, USA
[c] Heliospectra AB, Gothenburg, Sweden

ARTICLE INFO

Article history:
Received 18 December 2015
Received in revised form 30 April 2016
Accepted 2 June 2016
Available online 28 June 2016

Keywords:
Chlorophyll fluorescence
Photosynthesis dynamics
Fluorescence transient
Stress detection
Greenhouse illumination control
System identification

ABSTRACT

Artificial lighting control in industrial scale greenhouses has a large potential for increased crop yields, energy savings and timing in greenhouse production. One key component in controlling greenhouse lighting is continuous and accurate measurement of plant performance. This paper presents a novel concept for remote detection of plant performance based on the dynamics of chlorophyll fluorescence (CF) signals induced by a LED-lamp. The dynamic properties of the CF is studied through fitting a linear dynamic model to CF data. The hypothesis is that changes in photochemistry affects the fluorescence dynamics and can therefore be detected as changes in the model parameters and properties. The dynamics was studied in experiments using a sinusoidal varying light intensity (period 60 s) or step changes (step length 300 s). Experiments were performed in a controlled light environment on Basil plants acclimated to different light intensities. It is concluded that the capacity to use a certain light intensity is reflected by how fast and how complex the dynamics are. In particular, the results show that optimal model order is a potential indicator of light tolerance in plants that could be a valuable feedback signal for lighting control in greenhouses.

1. Introduction

Chlorophyll fluorescence (CF) is a widely used non-invasive probe of photosynthesis. The close relationship between CF and photosynthetic performance has made it an indispensable tool in studying photosynthesis in a wide range of applications on-leaf as well as remotely from satellites (Murchie and Lawson, 2013; Porcar-Castell et al., 2014). From lab-scale to ecosystem-level CF is used to detect stress caused by various types of stressors such as drought, nutrient deficiency, pests and excess light (Baker and Rosenqvist, 2004). Although at present not widely used in greenhouses, the potential of using CF for optimisation of greenhouse production has been pointed out by, for example, Baker and Rosenqvist (2004).

Photosynthesis in plants is driven by light energy absorbed by chlorophyll molecules within the photosynthetic apparatus. The absorbed light can be used to (i) drive photosynthesis (photochemistry), (ii) be dissipated as heat or (iii) be re-emitted as light (CF). These three processes compete for the absorbed light quanta and hence, fluorescence emission indirectly contains information about the quantum efficiency of photochemistry and heat dissipation (Murchie and Lawson, 2013). The heat dissipation is a protective mechanism induced in conditions when the excitation pressure on photosystem II (PSII) exceeds the rates of electron transport and carbon fixation. Thus, at low light conditions, the probability of fluorescence is negatively correlated with the probability of photochemistry, while at high light conditions it is turned into a positive correlation due to an increased probability of heat dissipation (van der Tol et al., 2009). The actual yields of photochemistry and heat dissipation, respectively, are generally sorted out from the fluorescence signal by so called fluorescence quenching analysis, described below.

CF has become a useful tool for studying photosynthesis mainly due to the invention of the pulse amplitude modulation fluorometer (PAM), which has the ability of extracting the yield of fluorescence (i.e., the probability of fluorescence) from noisy data in presence of background light (Schreiber, 2004). The PAM measures the CF response to short duration (micro seconds) light pulses and discriminates between CF induced by the excitation pulse from CF induced by ambient light through synchronous detection. The excitation light pulse is so weak that photochemistry and heat dissipation

* Corresponding author.
E-mail addresses: anna-maria.carstensen@chalmers.se (A.-M. Carstensen), pococt@rpi.edu (T. Pocock), daniel.bankestad@heliospectra.com (D. Bånkestad), tw@chalmers.se (T. Wik).

http://dx.doi.org/10.1016/j.compag.2016.06.002
0168-1699/

are considered unaffected during the pulse and, consequently, the yield of fluorescence can be determined by dividing the amplitude of the induced CF with the amplitude of the excitation pulse (Schreiber, 2004). Since the system is considered constant under the short interval of measurement, the frequency of modulation of the excitation light source does not affect the response (more than through increasing the integral of the excitation light). By measuring the fluorescence yield at different light intensities, (Fm) at short duration saturating light that transiently eliminate the photochemical yield, and (Fo) at extremely low light intensities where the photochemical yield is maximal, and comparing these through quotients, the rate constants for photochemistry, heat dissipation and fluorescence are sorted out and quantified (Govindjee, 2004). By doing so at different physiological conditions, such as dark adapted, light adapted or conditions caused by different types of stress, changes in heat dissipation and changes in photochemistry can be detected.

The PAM-technology has found numerous applications. Although best suited for on-leaf application, the PAM methodology has been adapted to remote sensing at different distances by using lasers for the fluorescence induction (Ounis et al., 2001; Moya and Cerovic, 2004). In remote sensing applications the main problem is to generate a saturating light for the measurement of Fm. Dark adaption for measuring the Fo level is another problem. In these applications, though, tracking the development of the steady state fluorescence yield has proven useful (Evain et al., 2004). The PAM technology has also been implemented in imaging systems for CF detection (Nedbal et al., 2000). These systems have found their use mainly for phenotyping (Gorbe and Calatayud, 2012). The PAM has also been modified for the use in commercial greenhouses. Schapendonk et al. (2006) have, with a modified PAM-equipment mounted fairly close to the plants, shown that fluorescence signals can be used for optimisation of light intensity in a greenhouse crop.

Photochemistry can also be studied based on the characteristic inflection points of the CF transient in dark-adapted leaves that are illuminated with continuous light. The inflection points on this transient are labelled OJIPSMT. During the initial fast phase of the induction curve (OJIP) chlorophyll fluorescence rises from the initial low origin level O, via the intermediate inflections J and I, to a peak level P in about 1 s, which is considered to reflect the successive reduction of the electron acceptor pool of PSII. During the subsequent slow phase (PSMT), the fluorescence declines to a terminal steady-state level T in the time-scale of minutes. The decline is often accompanied by a local, semi steady-state, minimum S and a local maximum M, and sometimes more than one pair of S and M inflections (oscillations) can be observed (Walker, 1992; Walker et al., 1983). The slow phase is more difficult to interpret as many different processes linked to photochemical quenching (qP) and non-photochemical quenching (NPQ) are known to influence the signal. The fast phase of this transient (OJIP) has been used for detecting drought in tomato plants remotely in a greenhouse by Takayama et al. (2011). However, their method requires dark adaption, and can thus only be used at night and not in daylight.

The aim with our research is ultimately to achieve an automatic and closed loop control of lighting in greenhouses, based on plant performance estimated from remotely sensed CF. For this we are aiming at a method for continuous estimation of plant health at daytime in a greenhouse. We propose a method that employs the dynamic properties of the remotely sensed light induced CF-signal. The dynamic properties of the CF is studied through the parameters in a linear dynamic model fitted to CF data. The hypothesis is that changes in photochemistry affects the fluorescence dynamics and can be detected as changes in the model parameters. Practically, we suggest this technique to be integrated into an advanced LED-lamp, where the LED-lamp induces fluorescence that is measured by a sensor in, or attached to the lamp. The sensor receives CF from the whole region of the plant canopy illuminated by the lamp, hence giving an aggregated and representative measure that could be used for feedback control of the LED lamp.

In the present work two different approaches to the study of CF dynamics are explored, namely frequency analysis and transient analysis. In the frequency analysis the fluorescence response to a sinusoidal varying light (period 60 s) was studied through linear analysis of the gain and phase shift. The frequency analysis has some similarities to analysis performed with a PAM. Similarly to the fluorescence yield measured by a PAM, the fluorescence gain discussed here is the quotient between the amplitude of the excited fluorescence divided by the amplitude of the excitation signal. However there are, two major differences between fluorescence yield and fluorescence gain. Fluorescence yield is excited by high frequency pulses of low amplitude, whereas fluorescence gain measured here is excited by low frequency harmonic modulations of high amplitude. The PAM method is assumed to maintain constant conditions under measurement (due to the weak excitation) such that no dynamics are exhibited in the fluorescence response, while the latter method do exhibit dynamics governing the gain as well as the phase. Furthermore, the dynamics imply that the frequency of modulation affects these values.

The dependency of the frequency of modulation is further explored through models of CF tranients. In the transient analysis the CF response to a step change in light intensity (step length 300 s) was analysed in terms of linear dynamic parametric black box models fitted to data. The analysis of the step responses constitutes a dynamic analysis of the PSMT transient in light adapted leaves.

Here we present some initial results based on light stress induction and recovery experiments performed on Basil plants acclimated to low, intermediate and high light. One of the key findings was that the intensity of the ambient light, in relation to the light intensity that the plants were acclimated to, determined how fast the plants responded to the step changes. Hence, light intensity shifted the plants' dynamic behaviour in the frequency domain. Even more interesting was that the complexity of the dynamics was decreased upon increased light intensity above the light intensity of acclimation. The complexity of the dynamics was also affected by light induced stress. The mechanisms behind these observations have the character of a buffer system with feedback, where the buffers are likely metabolite pools. These results were obtained from the analysis of black-box models of step responses. Interestingly, these results were also in agreement with the gain and phase shifts estimated from the experiments with sinusoidally varying light.

2. Materials and methods

2.1. Plant material and growth conditions

Ocimum basilicum (sweet basil cv. Nufar) was grown in five different growth units under different light settings. In three of the growth units the plants were grown under L4AS1 LED-lamps (Heliospectra, Sweden) with incident light intensity set to 80, 250 and 500 μmol photons m^{-2} s^{-1} respectively within PAR and with the spectral distribution presented in Fig. 1. In the two remaining growth units plants were grown under HPS-lamps (spectrum shown in Fig. 1) with the light intensity set to 80 and 500 μmol photons m^{-2} s^{-1} within PAR. These light intensities and spectral distributions were measured with a calibrated JAZ spectrometer (Ocean Optics, US) without plants in the units. The photoperiod was 16 h.

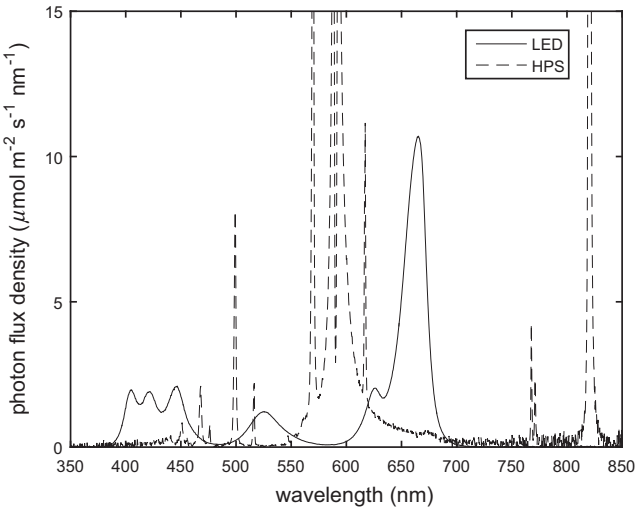

Fig. 1. Spectrum in the growth units with LED-lamps and HPS-lamps respectively. The two spectra are measured in growth units with the light intensity set to 500 μmol photons m^{-2} s^{-1} within PAR, but are representative for the other light intensities as well.

The plants were grown in a mix of 2 parts of standard potting soil and 1 part of Agra-Vermiculite (Pull Rhenen B.V., Netherlands). Osmocote (Osmocote Exact Mini 3–4 M, Everris) was added to the soil with 2 g/l as fertilizer. Additional fertilisation was supplied to the plants grown under 500 μmol photons m^{-2} s^{-1} at each watering with VITA-GRO TM, while keeping the nitrogen application at 200 ppm. The temperature in the growth units were 20–26 °C during day and 15 °C during night.

2.2. Stress induction and recovery experiments

Stress induction and recovery experiments were performed on whole plants with 2–4 fully expanded pair of leaves under the L4AS1 LED-lamp. Each experiment consisted of four phases with different background light intensity:

- Phase I: 110 μmol photons m^{-2} s^{-1} for 2.5 h.
- Phase II: 530 μmol photons m^{-2} s^{-1} for 1 h.
- Phase III: 1750 μmol photons m^{-2} s^{-1} for 2 h.
- Phase IV: 110 μmol photons m^{-2} s^{-1} for 3–6 h.

The background light in all four phases had the same spectral distribution as the LED growth light presented in Fig. 1. On top of the background light intensity an additional excitation light signal (see Section 2.3) generated by the LED-lamp was running throughout the whole experiment. The type of excitation signal (step or sinusoid) affected the mean value of the background light intensity slightly. During Phase I, II and IV of the experiment, sinusoidal excitation affected the background light intensities such that it became almost 40 μmol photons m^{-2} s^{-1} higher than the above presented intensities for the background light.

In between the experimental phases there were periods with no background light and only excitation signal. These periods were 5 min in the experiments with sinusoidal excitation and 10 min in the experiments with step excitation. Consequently, in the figures where these two experiments are compared over time (Figs. 13 and 14 in the Results section), the time axis for the step response experiments is shortened with 5 min between each experimental phase.

Continuously during the experiments incoming light, reflectance and fluorescence was measured remotely by spectrometers (see Section 2.5). Plant health was also regularly monitored through manual on-leaf measurements with a Pulse Amplitude Modulated fluorometer (PAM) (see Section 2.4), for comparison with the remote sensing results. The manual on-leaf measurements with the PAM affected the remotely sensed fluorescence signal, and therefore the experiment was repeated twice for each excitation signal on each set of plants, once with interruption for PAM measurements and once without.

The temperature was not controlled during the experiments and increased illumination gave rise to increased temperature. The temperature ranged between 22–24 °C during Phase I and IV of the experiment, 26 °C during Phase II and 34–37 °C during Phase III.

2.3. Excitation signals

Within the field of System Identification, an *excitation signal* is used to excite dynamic states in a system. The relation between the excitation signal and a measured output signal from the excited system is then analysed in terms of a dynamic model of the system. Here we use the concept excitation signal for describing a varying light intensity applied to induce variations in chlorophyll fluorescence.

Two different excitation signals were employed: (1) light varying between two levels, forming step increases and step decreases and (2) sinusoidal varying light. The excitation signal was, in both cases, generated by blue LEDs (peak maximum at 420 nm) in the LED-lamp. The step length was chosen to be 300 s, since that was the time it took for the transient fluorescence response to reach a steady state. The period of the sinusoid was 60 s. This periodicity was chosen based on a pre-study described in Wik et al. (2012). In that study transfer functions were estimated to step responses. Before the present study, these transfer functions for stressed and non stressed plants were plotted in a bode diagram, and the frequency causing the largest difference in gain between stressed and non stressed plants was chosen. Interestingly, fluorescence responses to this frequency has previously been studied by Nedbal (2003). Both a resonance peak and strong upper harmonic oscillations were reported to occur, not only in fluorescence but also in CO_2 capture, upon harmonically modulated light at this frequency ($\omega = 2\pi/60 \approx 0.1$ rad/s) (Nedbal, 2003).

The amplitudes of the excitation signals (defined as max–min) were 60 μmol photons m^{-2} s^{-1} for steps and 120 μmol photons m^{-2} s^{-1} for sinusoids as measured with the Jaz spectrometer at the canopy level in the absence of plants. This means that the step excitation signal affected the background light intensity with ±30% in Phase I and IV of the experiment, ±6% in Phase II and ±2% in Phase III. The corresponding alteration with sinusoidal excitation were ±40%, ±10%, and ±4%.

Experiments with sinusoid excitation was performed on all set of plants, while experiments with step excitation were only performed on plants acclimated to the LED-spectrum.

2.4. On-leaf PAM measurements

On-leaf CF measurements were made with a Pulse Amplitude Modulated chlorophyll fluorometer (JUNIOR-PAM; Heinz Walz; Effectrich, Germany) at room temperature on detached leaves. For this, the youngest fully expanded leaves from 3 to 4 plants randomly distributed in the experimental area were picked. Prior to measurements the leaves were dark adapted for a minimum of 20 min to fully oxidise QA. During the dark adaption leaves were stored on moist paper towel. Minimum fluorescence (Fo) was measured using weak blue (450 nm) measuring light pulses while maximum fluorescence (Fm) was measured after a saturating blue

(450 nm) light pulse of 10,000 μmol photons m^{-2} s^{-1} for 800 ms. The ratio Fv/Fm was used to indicate changes in the maximum efficiency of PSII photochemistry with Fv calculated as Fm–Fo (Krause and Weis, 1991).

2.5. Remote spectrometer measurements

During the experiments incoming light from the LED-lamp was measured at the canopy level by a calibrated Maya 2000 Pro Spectrometer (Ocean Optics, US) equipped with a 50 μm optical fibre and cosine corrector giving a field of view of 180°. Spectral radiance from the plant canopy (reflected light and fluorescence) was measured at a distance of 1 m from the plant canopy by a calibrated QE65000 spectrometer (Ocean Optics, U.S.) equipped with a 600 μm optical fibre with a field of view of 25° (see Fig. 2).

The collected spectral radiance originated from a canopy region forming a circle with a radius of approximately 22 cm. The canopy was diverse with multiple leaf layers and with leaves facing the lamp in different angles. This implied a variation in incident irradiance of individual leaves which probably caused a varying photosynthetic activity. The measured CF signal is therefore a superposition of signals emanating from leaves with different light history and different photosynthetic activity. However, since the sensor is positioned in between the two LED-lamps generating the excitation signal, we expect that the leaves contributing the most to the superposed signal are those that are the most affected by the LED-lamp. This justifies the method, that ultimately should be used for control of a LED-lamp.

The spectrometers were calibrated against a LS-1-CAL calibrated light source (Ocean Optics, U.S.). Data acquisition was carried out with a home-made software based on JAVA-modules containing the device drivers for the spectrometers available from Ocean Optics.

2.6. Calculations

Spectrometer data was corrected for electric dark currents and temperature effects in the spectrometers. Thereafter, absolute irradiance values (μmol photons m^{-2} s^{-1}) were calculated for each wavelength based on calibration coefficients. The intensity of the excitation signal at each time instance was then calculated as the integrated absolute irradiance (μmol photons m^{-2} s^{-1}) in the wavelength interval 380–480 nm, based on data collected with the spectrometer facing the lamp. For radiance data collected with the spectrometer facing the plants, integrated absolute irradiance was calculated for the interval 700–780 nm, representing the fluorescence signal with a maximum at 740 nm. The calculated integrated irradiances were then used as the input and output signals in the analyses of sinusoid and step responses.

2.6.1. Analysis of sinusoid responses

When a linear system is affected by a sinusoidal input the system's response to that input is also a sinusoid however, with a changed amplitude and phase. How much the amplitude and the phase are affected by the system is dependent of the frequency of the sinusoidal input. Whereas a linear system only affects the amplitude and the phase, a non linear system also modulates the frequency, such that the output signal becomes a sum of sinusoids of different frequencies.

The response to the sinusoid excitation was analysed linearly in terms of gain and phase shifts. Prior to the analysis the integrated irradiance data was detrended with a floating average running over a 60 s period. Thereafter sinusoids,

$$y = \theta_1 \sin\left(\frac{2\pi t}{60} + \theta_2\right) + \theta_3, \tag{1}$$

with the free parameters amplitude (θ_1), phase shift (θ_2) and offset (θ_3), were fitted by least squares to each period (60 s) of the input and output data. The sinusoids gave a close fit to data for both the excitation signal and the fluorescence signal, which motivated a linear analysis in terms of gain and phase shifts. The gain was then calculated as the amplitude of the fluorescence signal ($\theta_{1_{740}}$) divided by the amplitude of the excitation signal ($\theta_{1_{420}}$), i.e.,

$$\text{fluorescence gain} = \frac{\theta_{1_{740}}}{\theta_{1_{420}}}. \tag{2}$$

The phase shift was calculated as the difference between the phase of the fluorescence signal and the phase of the excitation signal, i.e.,

$$\text{phase shift} = \theta_{2_{740}} - \theta_{2_{420}}. \tag{3}$$

2.6.2. System identification of step responses

The step responses were analysed in terms of linear black-box models. These types of models are characterised by their model structure and their order. The general model structure is described by

$$y(t) = \frac{B(q)}{A(q)}u(t) + \frac{C(q)}{D(q)}e(t), \tag{4}$$

where t is time, $y(t)$ is the measured output (fluorescence), $u(t)$ is the input (the excitation signal) and $e(t)$ is noise (for example measurement noise from the spectrometer). A, B, C and D are

Fig. 2. Experimental set up consisting of a styrofoam box, two lamps, the plant canopy and the two optical fibres. One fibre is positioned at the plant canopy level and is collecting irradiance from the lamp. The other fibre is positioned between the two LED-lamps and is collecting radiance from the plant canopy. Photons from a circle of radius 22 cm of the plant canopy is collected by the optical fibre and passed to a spectrometer.

polynomials in the forward shift operator q and it is their polynomial degree that defines the model order. $B(q)/A(q)$ defines the process model, i.e., the model of the response of the photochemistry to changes in the incident blue light, whereas $C(q)/D(q)$ is a noise model. The order of the B-polynomial defines the number of zeros in the process model, while the order of the A-polynomial defines the number of poles in the process model.

From the general model structure in Eq. (4), model structures of different complexity can be obtained. The easiest model structure to compute is the ARX (Auto Regressive with eXogeneous input) model, obtained by letting $A = D$ and $C = 1$. The estimation of an ARX model, i.e., least squares determination of the parameters in A and B, forms a pure linear regression and therefore has an explicit and normally unique solution. If additional freedom in the modelling of the noise is added by a C-polynomial, the model structure is called ARMAX (Auto Resgressive Moving Average with eXogenous input). By instead letting $C = D = 1$, an OE (Output Error) model is obtained. If all the polynomials in Eq. (4) are estimated, the more complex BJ (Box–Jenkins) model structure is obtained. The estimation of an ARMAX, OE or a BJ model form pseudo linear regressions to be determined iteratively, giving a solution that may depend on initial guesses of the parameter values (Ljung, 1999).

The step responses were different for step increases and step decreases, implying that the system is nonlinear. This motivated separate model estimation to step increases and step decreases, while keeping the models linear. Hence, prior to the modelling, data was cut into steps up and steps down, with 60 s of data included before each change in level. For the work presented here only the responses to step increases were analysed. After interpolation of the data ($\Delta t = 0.2$ s), each step was linearly detrended, by subtracting a linear trend fitted to the base level before the step and the base level before the next step. The detrended data was resampled and during the process of resampling, an antialiasing (low-pass) FIR-filter of order 3 was applied.

The linear modelling was implemented through estimation of one new model to each step. The rational behind this procedure was to let the model parameters, within one selected model structure and order, adapt as the dynamics of the photosynthesis change due to altered physiology. Hence, the first part in the identification procedure was to find a model structure and model order applicable to all the four different phases in the experiment. Since the step responses under low light intensity, during Phase I and IV of the experiment, exhibited the most complex transients, the model structure and order was selected based on its suitability for modelling of the steps from these phases.

The search for a suitable model structure and model order followed the procedure described by Ljung (1999, Chapters 16 and 17). Iteratively, data was filtered to different extent, whereupon models of different orders within different model structures were estimated and evaluated. One or several step responses from Phase I of the experiment were selected as estimation data and the preceding and following step were selected as validation data. The estimated models were evaluated with emphasis on how well they could simulate the fluorescence transients, both on estimation data and on validation data. An evaluation was also performed in the frequency domain, by comparison of the parametric models with the non-parametric Empirical transfer function estimate (ETFE) in Bode diagrams. The evaluation in the frequency domain also covered convergence and the size of model uncertainties.

First ARX models of different orders were estimated and evaluated. For the ARX models, the fit in simulation improved slowly with increasing model order. At least 10 poles and 10 zeros were needed in order to capture essential features in the dynamics. However, investigation of the position of the poles and zeros of the ARX models showed that only around 3–4 poles and zeros were motivated. This indicated that the excess poles and zeros were used to improve the noise model and that another structure of the noise model would be more appropriate. Hence, ARMAX, OE and BJ models of different orders were tested. All these model structures needed at least 3 poles and zeros for performing well in simulation. With more than 4 poles and 4 zeros, pole-zero cancellations were obtained. An OE model with 3 poles and 3 zeros gave the best results in simulation on both estimation data and validation data, independently of the prefiltering of the data. With reduced low pass filter bandwidth the behaviour of the ARMAX, OE and BJ models with 3 poles and 3 zeros gave very similar results in terms of fit in simulation, Bode plots and pole-zero-positions. The most robust results for all steps in the experiment were obtained for the OE model when the data was filtered and resampled to a sampling interval of $\Delta t = 2$ s. Since the estimation of an OE model needs initial guesses of the parameters, the estimation of a model to one step was initialised by the parameter values obtained from the previous estimated model. This was done iteratively for each experimental phase, starting by estimating a model to the first step in one phase and proceeding to the last step by using the previous step for initialising the estimation of the next. Thereafter the order for the estimation was reversed, using the last model as initialisation for the previous one. Estimation and evaluation of models were carried out using System Identification Toolbox in MATLAB (Ljung, 2007).

3. Results and discussion

3.1. Stress induction and Fv/Fm

Plants acclimated to different light intensities (80, 250 and 500 μmol photons m^{-2} s^{-1}) and spectra (LED and HPS) responded differently to the light treatment of the experiment (Phase I, II, III and IV with 110, 530, 1750 and 110 μmol photons m^{-2} s^{-1} respectively) as can be seen from the Fv/Fm values presented in Fig. 3. As expected, the plants grown at low light (80 μmol photons m^{-2} s^{-1}) were more susceptible to light induced stress relative to the plants grown at moderate light (250 μmol photons m^{-2} s^{-1}) as observed by the decreases in Fv/Fm (Fig. 3A). Initially, i.e., during Phase I, Fv/Fm for the plants grown at low light decreased slightly, possibly because of the moderate increase in light (from 80 to an average of 150 μmol photons m^{-2} s^{-1}), while no trend can be observed for the others. The Fv/Fm values during Phase I for plants grown under high light (500 μmol photons m^{-2} s^{-1}) were variable (Fig. 3B). This

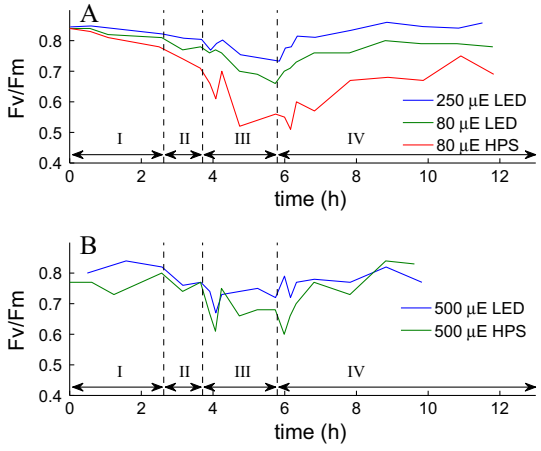

Fig. 3. Fv/Fm measured during the experiment consisting of four Phases on plant material acclimated to different light intensities and spectrum as indicated in the graph. The figure shows the mean value of on leaf measurements on four leaves. The presented Fv/Fm values were measured during experiments with sinusoids as excitation signal.

could be due to that the PAM only measures a very small point on the leaf, combined with different rates of acclimation to the low light and lack of growth-light uniformity due to a denser canopy and larger variation in morphology.

During Phase II and III all plants decreased in Fv/Fm but to different extent. Interestingly, plants grown at low light under the LED spectrum were more tolerant to photoinhibition than those grown under HPS. The Fv/Fm values for plants acclimated to the low light LED-spectrum decreased by 19% from the level in the end of Phase I, whereas there was a 28% decrease in Fv/Fm for plants acclimated to the low light HPS-spectrum (Fig. 3A).

All plants recovered at low light during Phase IV (Fig. 3A and B). The slowest recovery was observed in plants acclimated to low light with HPS-spectrum (Fig. 3A). Their recovery was not fully completed in the course of the experiment (6 h of recovery). All the other set of plants recovered in less than 3 h to at least the Fv/Fm value they had at the end of Phase I.

The type of excitation signal used during the experiment (sinusoid or step) was not found to affect the trends observed in Fv/Fm (data not shown). Furthermore there were no significant difference in how plants responded to the light treatment when the experiment was repeated after a few days of re-acclimation of the plants to their normal light environment. Hence, previous light events did not confer tolerance to future light stresses as one might expect. Therefore, the Fv/Fm values presented are seen as representative also for experimental days when no Fv/Fm values were recorded.

3.2. Results with sinusoid excitation

The remotely detected fluorescence response to the sinusoidal excitation signal, did have a shape very close to a sinusoid (Fig. 4), implying that under the experimental conditions described here, the system can be treated as nearly linear. The reason for the linear behaviour could be that the amplitude of the variation in light intensity due to the excitation signal is quite small (±60 μmol photons m^{-2} s^{-1}) and could be seen as variations around an operating point, where the system behaves approximately linearly. The most non-linearities where found in Phase I when the background light intensity was 110 μmol photons m^{-2} s^{-1}. Due to

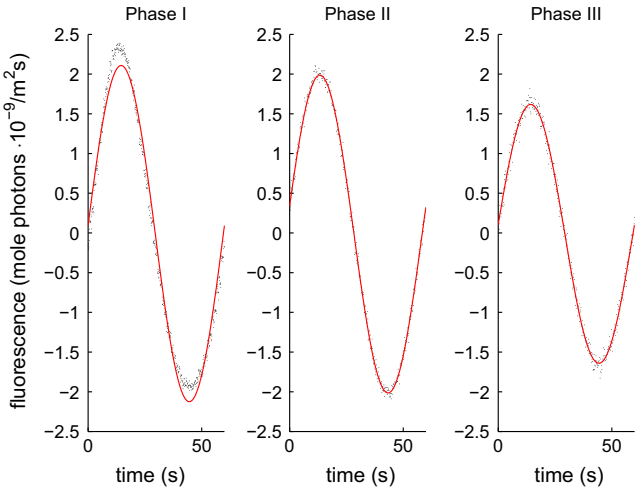

Fig. 4. Detrended absolute irradiance measured remotely by a spectrometer and integrated over the wavelength interval 700–780 nm representing fluorescence intensity (black dots) together with a sinusoid fitted to data in a least square sense (red line). From left to right one period from each of Phase I, II and III of the experiment. The response plotted for Phase I is representative also for Phase IV. Data collected from plants acclimated to 80 μmol photons m^{-2} s^{-1} and LED spectrum. (For interpretation of the references to colour in this figure legend, the reader is referred to the web version of this article.)

the close to linear fluorescence response, linear analysis was carried out through determination of the gain and phase shift for each period (60 s).

3.2.1. Fluorescence gain

The fluorescence gains, determined according to Eq. (2), for the five sets of plants grown under different light treatments are shown in Figs. 5 and 6. These figures also contain the Fv/Fm values (earlier presented in Fig. 3) for comparison. Within each phase of the experiment the fluorescence gain exhibits slow continuous changes, whereas in the transition between the phases the gains respond instantly (within the first 60 s measuring period) to the changed background light intensity.

The slow continuous changes in the fluorescence gain agree with the changes in the Fv/Fm and are probably due to decreased variable fluorescence caused by increased heat dissipation and photoinhibition. This interpretation is motivated by the successive decreases in the gain observed for the plants during exposure to light intensities above their acclimation light, as in low light plants during Phase II and III (Fig. 5A and B) and in high light plants in Phase III (Figs. 5D and 6). This is also in accordance with that the gain increases during recovery at low light in Phase IV (Figs. 5 and 6).

The increase in light intensity in the transition from Phase I (110 μmol photons m^{-2} s^{-1}) to Phase II (530 μmol photons m^{-2} s^{-1}), brought on an instant increase in the fluorescence gain for all sets of plants. This instant increase is most clearly expressed for the plants acclimated to the Phase II light (Fig. 5C and D) as well as for plants acclimated to 250 μmol photons m^{-2} s^{-1} (Fig. 6), but appears also for the plants acclimated to 80 μmol photons m^{-2} s^{-1} (Fig. 5A and B). Differently, the increase in light at the beginning of Phase III (1750 μmol photons m^{-2} s^{-1}), brought on an instant decrease in the fluorescence gain for all sets of plants (Figs. 5 and 6).

The instant changes in the fluorescence gain upon changes in the background light intensity are most likely governed by changes in the yields of photochemistry and heat dissipation. Since these yields were not measured the interpretation given here is very speculative. Due to the fairly high amplitude of the excitation signal one might expect that the yields of photochemistry and heat dissipation are varying during one period (60 s) of the excitation signal. If the photochemical yield varies due to the modulation in light, one would expect a higher gain in the fluorescence, than if the photochemical yield is assumed constant. This effect would be due to that increasing light means decreasing photochemical yield and increasing fluorescence yield. A high fluorescence gain would then be indicative for a high variability in the photochemical yield. On the other hand, a high variability in NPQ would rather decrease the fluorescence gain. Since both the photochemical yield and the NPQ would vary dynamically their effect on the gain would be dependent of the frequency of modulation of the light. Given that this interpretation holds, low light acclimated plants have high variability in photochemical yield in Phase I, whereas high and moderate light acclimated plants have a high variability in photochemical yield in Phase II, thus, suggesting that a high gain and a high variability in photochemical yield are obtained at light intensities close to the light intensity plants have been acclimated to. Furthermore, the decrease in the gain observed in Phase III would within this hypothesis likely be due to a decrease in the variability of the photochemical yield caused by saturation probably combined with an effect of increased yield of heat dissipation.

3.2.2. Phase shifts

The phase shift of the fluorescence response to the sinusoidal varying light of angular frequency $\omega = 0.1$ rad/s, is determined for each period (60 s) according to Eq. (3). Figs. 7 and 8 show how the phase shifts vary during the experiment. The figures show

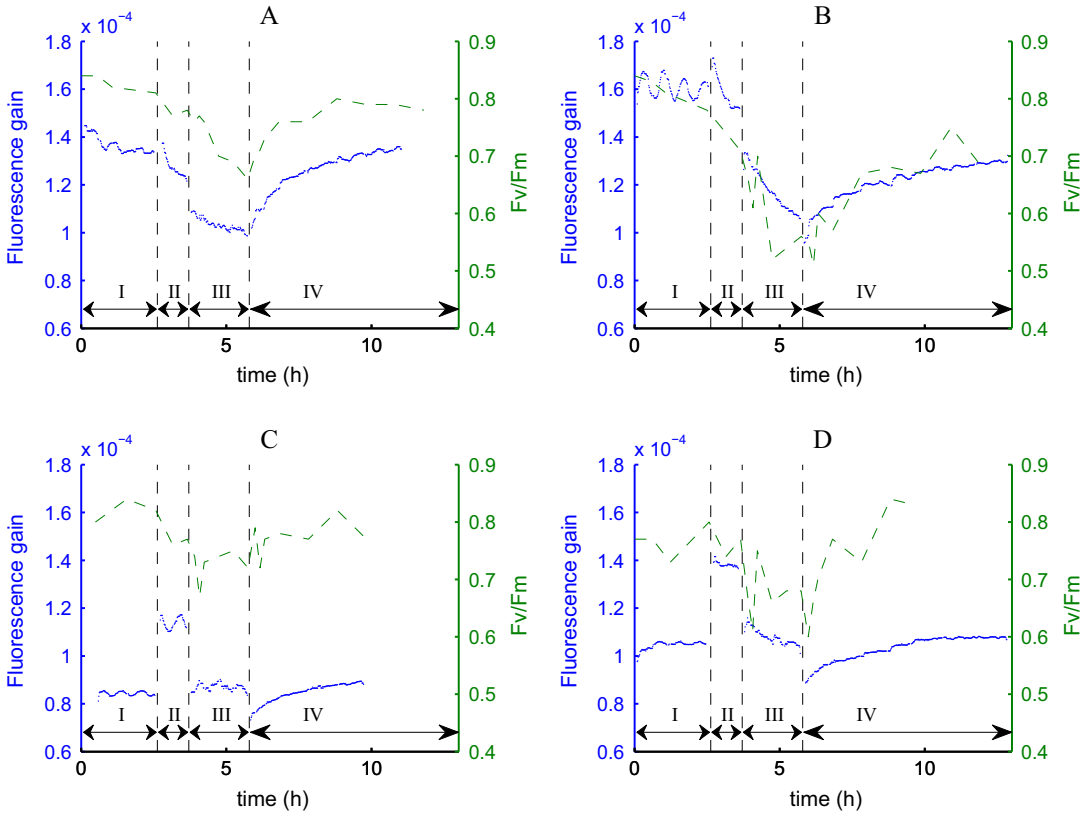

Fig. 5. Fluorescence gain and Fv/Fm from plants acclimated to 80 μmol photons m^{-2} s^{-1} and the LED spectrum (A), 80 μmol photons m^{-2} s^{-1} and the HPS spectrum (B), 500 μmol photons m^{-2} s^{-1} and the LED spectrum (C) and 500 μmol photons m^{-2} s^{-1} and the HPS spectrum (D). The oscillations in the fluorescence gain are due to temperature variations in the lab.

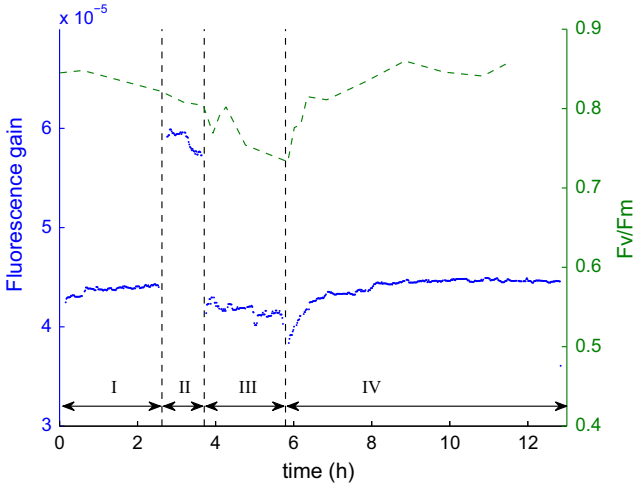

Fig. 6. Fluorescence gain and Fv/Fm from plants acclimated to 250 μmol photons m^{-2} s^{-1} and the LED spectrum.

that the phase shifts depend on both acclimation and background light intensity in an intricate way. Both positive and negative phase shifts were observed. A positive phase shift theoretically corresponds to that the photosynthesis partially responds proportionally to the derivative of the excitation signal and a negative phase shift corresponds to that photosynthesis partially responds proportionally to the integral of the excitation light.

Whether the observed phase shifts are positive or negative is determined by the background light intensity in relation to what light intensity the plants are acclimated to. Negative phase shifts were only observed for plants shifted to a lower light intensity than they were grown under. For plants under the light intensity they were grown under or higher intensities, the phase shifts were entirely positive. Furthermore, a decrease in the absolute value of the phase shifts was related to a decrease in Fv/Fm, whereas an increase in the absolute value of the phase shifts was related to an increase in the Fv/Fm. For example, the phase shifts for the plants acclimated to 80 μmol photons m^{-2} s^{-1} (Fig. 7A and B) were positive and decreasing while the Fv/Fm was decreasing during Phase I and positive but increasing during recovery of Fv/Fm during Phase IV. Phase II and III for these plants constitute an exception to this trend. For the plants acclimated to 500 μmol photons m^{-2} s^{-1} (Fig. 7C and D), the phase shifts were negative and decreasing during Phase I and IV, where the Fv/Fm value was increasing. For these plants the phase shifts became positive when the background light intensity was increased during Phase II and III. During these Phases and for these plants, the phase shifts were decreasing in parallel with the Fv/Fm. These somewhat contradictory findings will find an explanation in the analysis of the step response experiments presented in Section 3.3.2 and are further discussed in Section 3.4.

The phase shifts shows one major advantage compared to the fluorescence gain since they proved to be more robust in amplitude when comparing different experimental days with each other. The reason is that the phase shifts are an intensive measure that is not affected by leaf area and distance, etc. Determining the phase shifts from the measured fluorescence signal might also be less sensitive to disturbances, than computing the gain. However, the phase shifts might be hard to interpret based on the response to only one frequency. This could potentially be solved by superposition of a few frequencies.

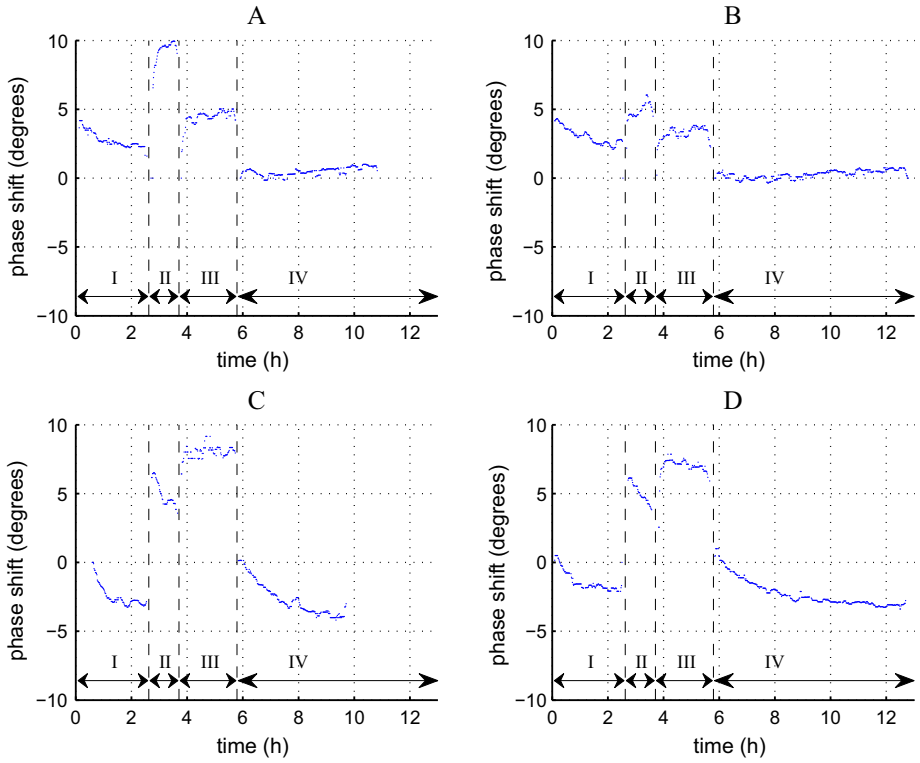

Fig. 7. Phase shifts in the fluorescence signal for plants acclimated to 80 μmol photons m^{-2} s^{-1} and the LED spectrum (A), 80 μmol photons m^{-2} s^{-1} and the HPS spectrum (B), 500 μmol photons m^{-2} s^{-1} and the LED spectrum (C) and 500 μmol photons m^{-2} s^{-1} and the HPS spectrum (D).

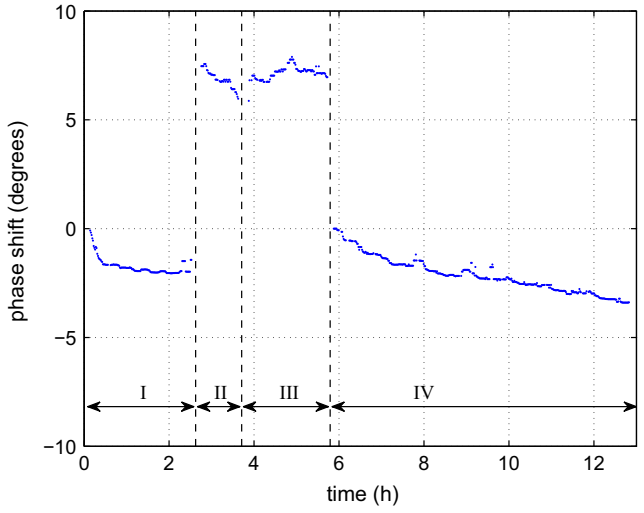

Fig. 8. Phase shifts in the fluorescence signal for plants acclimated to 250 μmol photons m^{-2} s^{-1} and the LED spectrum.

3.3. Results with step excitation

The fluorescence response to step excitation was different for step increases and for step decreases, implying that the system is nonlinear. Therefore, the analysis of the step responses were separated into linear analysis of step increases and step decreases respectively. Presented here are only the results for step increases.

As can be seen in Fig. 9, the fluorescence transients differ between different phases of the experiment. Furthermore, during recovery from stress (Phase IV) the transients are gradually changed. The responses also differ between plants acclimated to different light intensities. During Phase I the transients contain 2 peaks, that based on their occurence in time are interpreted as the P and M inflection points in the PSMT-tranisent. The first peak (P) is less pronounced and occurs after 1 s. The second peak (M) occurs after 8 s for plants acclimated to 80 μmol photons m^{-2} s^{-1}, after 26 s for plants acclimated to 250 μmol photons m^{-2} s^{-1} and, after 30 s for plants acclimated to 500 μmol photons m^{-2} s^{-1}. When the light intensity is increased to 500 μmol photons m^{-2} s^{-1}, during Phase II of the experiment, the first peak (P) becomes more pronounced while the second peak (M) disappears, except for the plants acclimated to this light intensity, for which the second peak is only suppressed but occurs earlier, after 8 s. The increased light intensity during Phase III also suppresses the first peak (P) slightly. When the plants are exposed to the lower light intensity again, during Phase IV, the two peaks (P and M) are suppressed compared to Phase I, but as Fv/Fm recovers both peaks become more pronounced.

Although the fluorescence transients studied here are measured from light adapted canopies, a comparison with slow fluorescence transients from dark adapted leaves reveals similarities in some respects. While low excitation light gives a transient with two peaks (P and M), high excitation light gives only one peak (P) (Strasser and Srivastava, 1995; Kalaji et al., 2012), which is similar to the transients from light adapted canopies presented here. However, contrary to transients from dark adapted leaves, the second peak (M) is generally higher than the first peak (P) in the transients presented here. This difference might be due to that the plastoquinone pool is not fully oxidised in the light adapted canopy.

3.3.1. System identification

The step responses were analysed in terms of linear black-box models. Models within different model structures and of different orders were estimated and evaluated as described in Materials and Methods. The focus in the identification work was to find a model structure and model order applicable to all the four phases in the

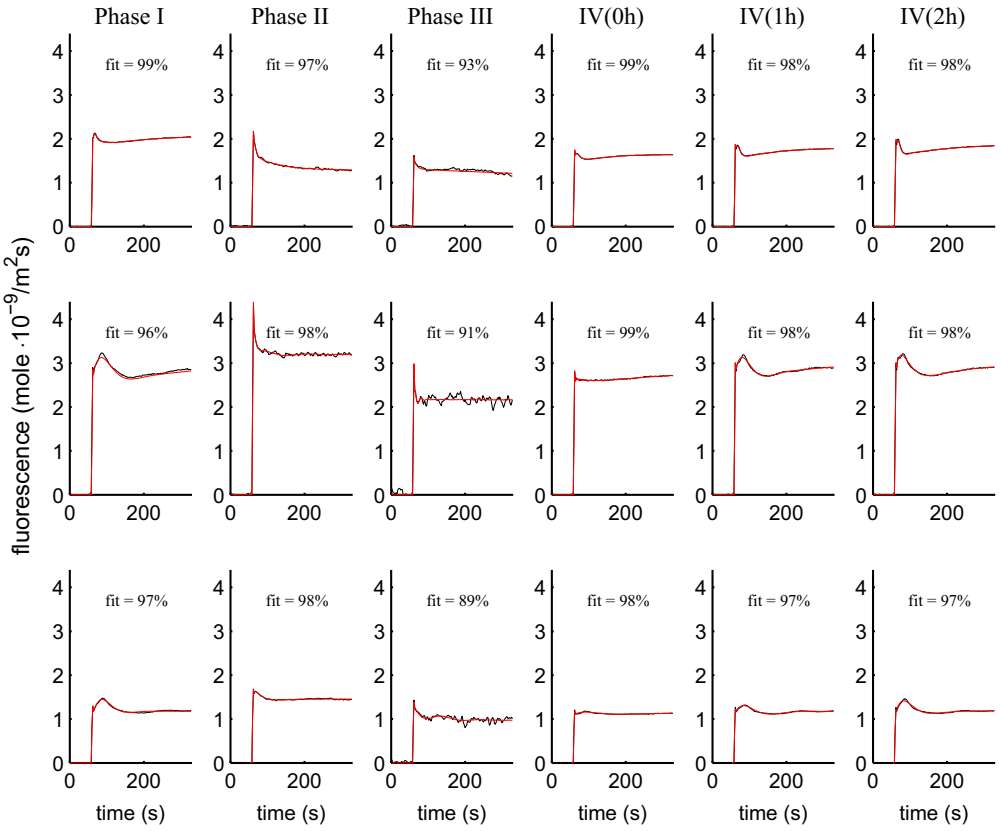

Fig. 9. Fluorescence response to step increases from plants acclimated to the LED spectrum and a light intensity of 80 μmol photons m^{-2} s^{-1} (top row), 250 μmol photons m^{-2} s^{-1} (middle row) and 500 μmol photons m^{-2} s^{-1} (bottom row). The figure shows from left to right one step from each of Phase I, Phase II and Phase III and 3 steps from Phase IV: first step during recovery, after 1 h of recovery and after 2 h of recovery. Filtered raw data (black) and simulated data (red) in the same graph. Normalized mean squared errors in the simulated model output compared to the measured data are indicated as fit in percentage. (For interpretation of the references to colour in this figure legend, the reader is referred to the web version of this article.)

experiment. The resulting model was an output error model with 3 poles and 3 zeros, i.e.,

$$y(t) = \frac{b_1 + b_2 q^{-1} + b_3 q^{-2} + b_4 q^{-3}}{1 + a_1 q^{-1} + a_2 q^{-2} + a_3 q^{-3}} u(t) + e(t) \quad (5)$$

A model of this structure and order was then estimated to each step response in the experiment. The resulting simulated fluorescence responses for steps from the different phases of the experiment are included in Fig. 9.

The system identification work started from the hypothesis that changes in parameter values or the position of poles and zeros could be used to track stress levels in plants. However, it turned out that both light intensity and stress level not only affected the parameter values but also the complexity of the dynamics, implying that different model orders are suitable for the modelling of plants under different background light intensities. For plants under low light a model with 3 poles and 3 zeros was motivated, whereas under higher light intensity this model order gave rise to cancellations between poles and zeros, implying that a lower model order is more suitable. This conclusion was further strengthened by the observation that some parameter values dropped to almost zero, as the light intensity was increased. The loss of complexity upon stress or increased light intensity made it inconvenient to track plant stress through these values. This is not only because the loss of complexity gave rise to jumps in the parameter values but also because their uncertainties increased when complexity was lost.

A more useful indicator of stress level in plants was the frequency function (see next section). The frequency function is obtained by replacing the time shift argument q in the system model by e^{iw}, and is written as

$$G(e^{iw}) = \frac{b_1 + b_2 e^{-iw} + b_3 e^{-2iw} + b_4 e^{-3iw}}{1 + a_1 e^{-iw} + a_2 e^{-2iw} + a_3 e^{-3iw}}. \quad (6)$$

The frequency function can be visualised in a Bode plot, showing the absolute value of the frequency function and the argument of the frequency function versus frequency. The advantage of the frequency function was that it proved to be less sensitive to model order, since it generally converged with increased model order.

3.3.2. Results in the frequency domain

The study of the fluorescence transients in the frequency domain revealed three main features relating to acclimation, light intensity and stress, respectively.

Acclimation to different light intensities affected how fast the dynamics of the fluorescence response was. The step responses from plants acclimated to 80 μmol photons m^{-2} s^{-1}, 250 μmol photons m^{-2} s^{-1} and 500 μmol photons m^{-2} s^{-1} were similar in shape, but the step responses from plants grown under 80 μmol photons m^{-2} s^{-1} were significantly faster (Fig. 10, left graph). In the frequency domain the faster dynamics exhibited by the low light acclimated plants corresponds to a shift of the frequency function towards higher frequencies (Fig. 10, the two graphs to the right).

Light intensity affected the fluorescence dynamics such that increased light intensity made the fluorescence dynamics faster, shifting the frequency function towards higher frequencies, as shown in Fig. 11. This behaviour was clear for the plants acclimated to 250 μmol photons m^{-2} s^{-1} and 500 μmol photons m^{-2} s^{-1}.

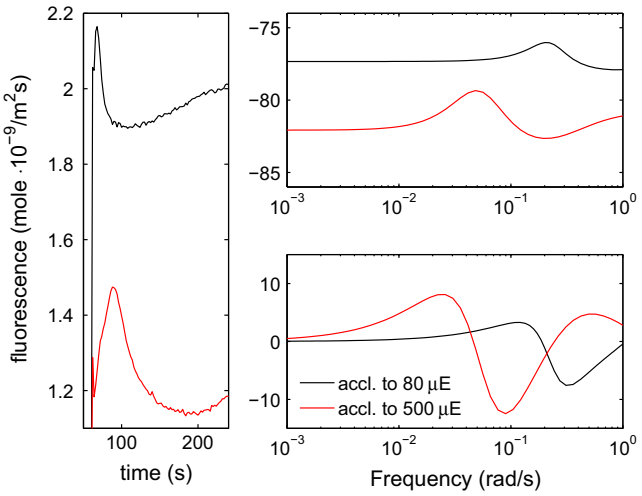

Fig. 10. Response from plants subject to 110 µmol photons m^{-2} s^{-1}, acclimated to different light intensities: 80 µmol photons m^{-2} s^{-1} (black) and 500 µmol photons m^{-2} s^{-1} (red). To the left: measured and filtered fluorescence step responses versus time. To the right: modelled step responses in the frequency domain, seen in a Bode diagram. (For interpretation of the references to colour in this figure legend, the reader is referred to the web version of this article.)

However the same behaviour was not found for the plants acclimated to 80 µmol photons m^{-2} s^{-1}. Furthermore increased light intensity led to more trivial dynamics as already discussed.

Decreased Fv/Fm made the dynamics less complex in the frequency range studied here. Fig. 12 shows how the frequency function was changed during recovery of Fv/Fm under 80 µmol photons m^{-2} s^{-1}. During recovery the complexity of the dynamics was successively increased, demonstrated by the increased resonance peak and increased phase shifts. The increased complexity of the dynamics gained during the recovery could also be seen through the pole-zero placements of the identified models. During recovery, poles and zeros lying close to each other diverged (data not shown).

The observed behaviour, where the flow of energy (light intensity) in relation to the capacity of utilising energy (due to acclimation) determines how fast the system responds to an input signal, is typical for a system consisting of buffer volumes. For a system of buffers, the response to an input signal becomes faster if the flow through the system is increased. The response also becomes faster for a buffer system with smaller volumes, i.e., a system with lower capacity, compared to one with larger. Furthermore, as the capacity of one or several buffers in a buffer system is reached the system will lose states, corresponding to a loss in complexity and system order. This is also a phenomena observed here through the pole-zero cancellations occurring when the light intensity is too high compared to the plants capacity. Although a buffer system alone would not give rise to any resonance peaks, this can be obtained by introducing feedback into the buffer system. Hence, we suggest that the mechanisms behind our observations have the character of a buffer system with feedback.

The mechanisms relevant for the timescale or frequency range (0.01–1 rad/s) studied here are, according to Eberhard et al. (2008), related to changes in electron flow, energy dependent NPQ, state transitions and enzymatic processes. Furthermore, the mechanisms that governs the slow fluorescence transient in dark adapted leaves are probably relevant to describe the slow fluorescence transient also in light adapted leaves to some extent. The slow fluorescence transient in dark adapted leaves exhibiting the PSMT pattern can only be obtained from intact chloroplasts (Papageorgiou et al., 2007) and depends on the whole electron transport process as well as the dynamics of carbon metabolism (Zhu et al., 2013). Moreover Nedbal (2003) has shown that

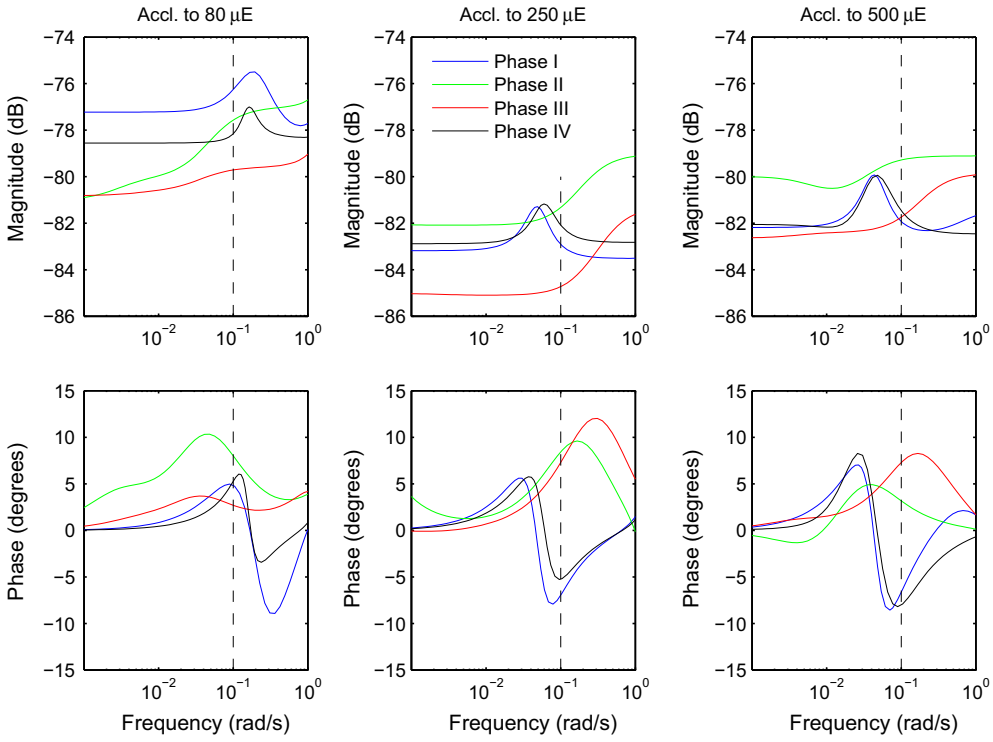

Fig. 11. Bode diagrams showing the mean value of the frequency functions from the different phases of the experiments. From left to right plants acclimated to 80 µmol photons m^{-2} s^{-1}, 250 µmol photons m^{-2} s^{-1} and 500 µmol photons m^{-2} s^{-1}.

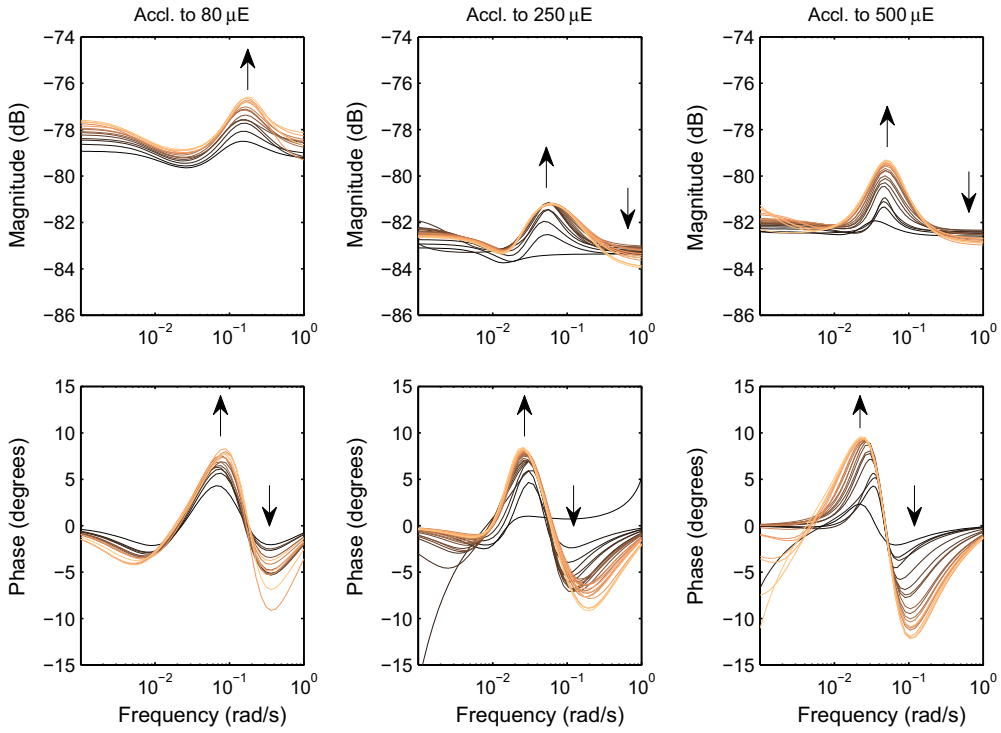

Fig. 12. Bode diagrams showing recovery from stress under 80 µmol photons m^{-2} s^{-1} in Phase IV of the experiments. From left to right plants acclimated to 80 µmol photons m^{-2} s^{-1}, 250 µmol photons m^{-2} s^{-1} and 500 µmol photons m^{-2} s^{-1}. The colour-scale goes from black to yellow with black indicating the beginning of Phase IV and yellow the end. Arrows indicate recovery. (For interpretation of the references to colour in this figure legend, the reader is referred to the web version of this article.)

harmonically modulated light within the frequency range of 0.02–0.3 rad/s causes oscillations not only in fluorescence but also in the CO_2 assimilation rate as well as in NPQ and in the effective quantum yield of PSII. This implies that the processes governing CO_2 assimilation and NPQ are affected by an input signal within this frequency range and that these processes further affects fluorescence transients. This suggests that the buffers affecting the models presented here are metabolite pools, e.g., ferredoxin, $NADP^+$, ADP, inorganic phosphate, 3-phosphoglyceric acid, ribulose-1,5-bisphosphate and hexosephosphates. The feedback mechanisms within the buffer system could be the regulation of NPQ and regulation of the CO_2 assimilation as well as regulation of cyclic electron transport and photorespiration. To further support our results, the metabolite pool sizes must depend on light acclimation. This would however be natural, since the higher light intensity plants are grown under, the higher capacity is needed for turning light energy into carbohydrates, meaning that larger metabolite pools are needed.

3.4. Comparison of results with step and sinusoid excitation

The results from the experiments with sinusoidal varying light alone were somewhat hard to interpret, in particular the phase shifts. Fortunately, the frequency domain results from the step responses provides an explanation. The frequency functions presented in Figs. 10 and 11 showed that the background light intensity in relation to the light intensity the plants are acclimated to determined the position of the frequency function. This clearly explains why the phase shift and the amplification of an input signal of a fixed angular frequency ($\omega = 0.1$ rad/s) could vary significantly depending on the plant material and background light intensity. According to the Bode plots for the plants acclimated to 500 and 250 µmol photons m^{-2} s^{-1} and Phase I of the experiment (see Fig. 11), an input signal of frequency $\omega = 0.1$ rad/s will result in a negative phase shift. However, the corresponding Bode plot for the plants acclimated to 80 µmol photons m^{-2} s^{-1} is shifted towards higher frequencies, resulting in a positive phase shift for an input signal of $\omega = 0.1$ rad/s. This is in agreement with the phase shifts presented in Figs. 7 and 8. When the light intensity is increased, also the Bode plots for the plants acclimated to 500 and 250 µmol photons m^{-2} s^{-1} are moved towards higher frequencies and consequently, the sinusoid of frequency $\omega = 0.1$ rad/s becomes positively phase shifted. Moreover, the instant changes in the fluorescence gain upon changed background light intensity (see Figs. 5 and 6) could to some extent be explained by movements of the position of the resonance peak in the Bode diagrams (Fig. 11).

A direct comparison of the step response models evaluated at $\omega = 0.1$ rad/s and the response to the sinusoid excitation is presented in Figs. 13 and 14. The gain and the phase shifts estimated from the sinusoid responses shows qualitatively high consistency with the step response models at this frequency. However quantitative differences exist, primarily in the phase shifts. The quantitative differences in the phase shifts are largest under Phase I and Phase IV of the experiment, which is also where the fluorescence response exhibited most nonlinearities (see Fig. 4). The differences would therefore be emphasised since the step response models are only estimated to step increases. Hence, the results based on sinusoid excitation and step excitation are affected by non linearities in different ways.

The oscillatory behaviour observed for the step responses in Figs. 13 and 14A, is related to temperature oscillations in the laboratory. The problem of temperature sensitivity could possibly be solved through system identification with multiple inputs, using the temperature as one input signal.

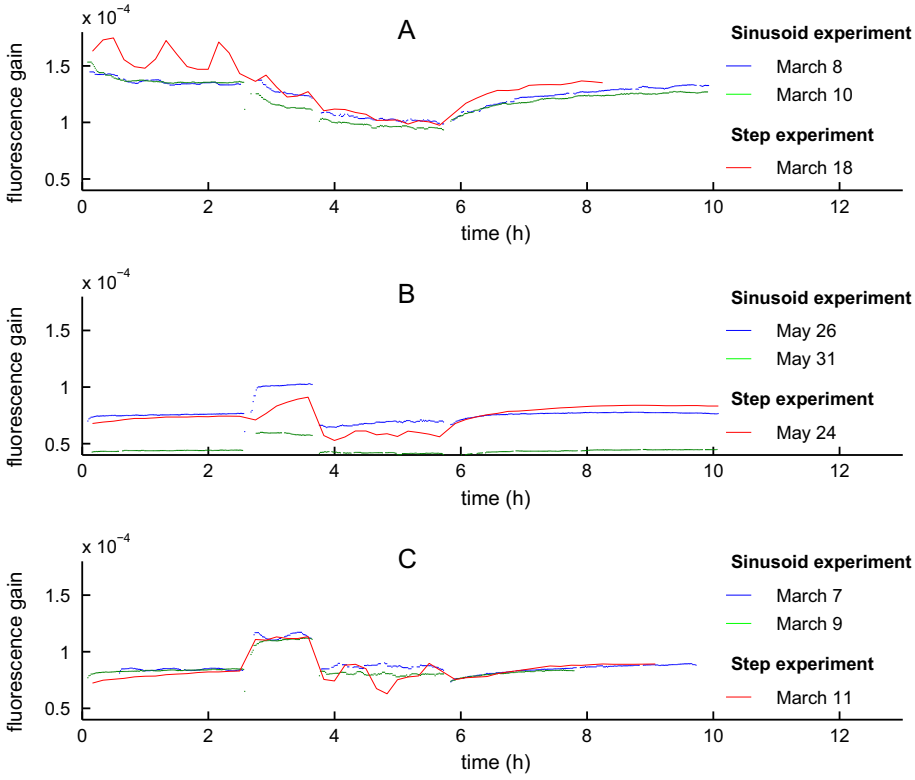

Fig. 13. Fluorescence gain at $\omega = 0.1$ rad/s for the experiments with sinusoids and for the transfer functions estimated from step responses on plants acclimated to the LED-spectrum of intensity (A) 80 μmol photons m^{-2} s^{-1}, (B) 250 μmol photons m^{-2} s^{-1} and (C) 500 μmol photons m^{-2} s^{-1}.

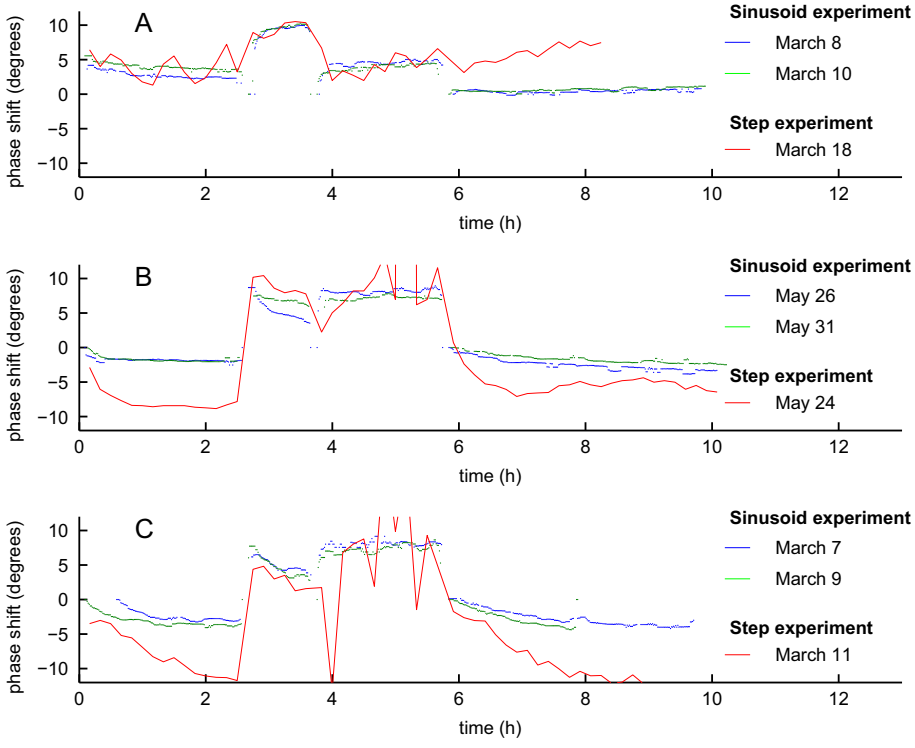

Fig. 14. Phaseshifts at $\omega = 0.1$ rad/s for the experiments with sinusoids and for the transfer functions estimated from step responses on plants acclimated to the LED-spectrum of intensity (A) 80 μmol photons m^{-2} s^{-1}, (B) 250 μmol photons m^{-2} s^{-1} and (C) 500 μmol photons m^{-2} s^{-1}.

4. Conclusion

The aim of the present study was to explore how the dynamics in photosynthesis, as revealed by remotely sensed fluorescence from plants, is affected by light intensity and light induced stress. This aim was based on the hypothesis that changes in the dynamics of the fluorescence signal can be utilised for remote detection of light use efficiency and plant stress at canopy level in a greenhouse. Ultimately, robust detection of these parameters could serve as control inputs for automatic and closed loop control of LED-lighting in commercial greenhouses which could lead to energy savings and increased crop yields.

The dynamics of the fluorescence signal was studied through frequency- and transient-analysis in experiments where plants acclimated to different light intensities and spectra were exposed to low light, intermediate high light and excess light. One of the key findings was that the background light intensity in relation to the light intensity that the plants were acclimated to determined how fast the plants responded to an excitation signal. Hence, light intensity shifted the plants dynamic behaviour in the frequency domain. Even more interesting was that the complexity of the dynamics was decreased upon increased light intensity above the light intensity of acclimation. The complexity of the dynamics was also affected by light induced stress. The mechanisms behind these observations have the character of a buffer system with feedback, where the buffers are likely metabolite pools. These results were obtained from the analysis of black-box models of step responses. Interestingly, these results were also in agreement with the gain and phase shifts obtained with sinusoid excitation.

In effect, these results opens up for new ways for remote detection of light use efficiency and light induced stress. Probably the most promising application of these results, is to utilise the loss of complexity upon increased light intensity as an indication of when plants maximum capacity for light utilisation is reached. Another technique could be based on the detection of how sinusoids of a few well selected frequencies are phase shifted. Such a method could be convenient in a noisy environment from a signal processing point of view. Both these methods would yield measures of photosynthesis that are intensive, i.e., unaffected by extensive parameters such as leaf area and distance. Yet another method could be to choose a frequency that yields a resonance peak in the fluorescence signal at a chosen working point, e.g., optimal photosynthesis rate. Although based on dynamical features of the photosynthesis, this latter method might be affected by extensive parameters as well.

Acknowledgements

The financial support for the work presented here came from Mistra Innovation (http://www.mistrainnovation.se). The experimental work was carried out in the laboratory at Heliospectra AB (Gothenburg, Sweden), and we are very thankful to the helpful and experienced co-workers in the lab. The authors are indebted to Erik Carstensen who wrote the software for the spectrometers, and to Julio César and Sina Soukhakian who wrote the software for the lamps. We are also thankful to Jonas Sjöberg (Chalmers University of Technology) for insightful comments on the system identification work.

References

Baker, N.R., Rosenqvist, E., 2004. Applications of chlorophyll fluorescence can improve crop production strategies: an examination of future possibilities. J. Exp. Botany 55 (403), 1607–1621.

Eberhard, S., Finazzi, G., Wollman, F.-A., 2008. The dynamics of photosynthesis. Ann. Rev. Gen. 42, 463–515.

Evain, S., Flexas, J., Moya, I., 2004. A new instrument for passive remote sensing: 2. Measurement of leaf and canopy reflectance changes at 531 nm and their relationship with photosynthesis and chlorophyll fluorescence. Remote Sens. Environ. 91 (2), 175–185.

Gorbe, E., Calatayud, A., 2012. Applications of chlorophyll fluorescence imaging technique in horticultural research: a review. Sci. Hortic 138, 24–35.

Govindjee, G., 2004. Chlorophyll a fluorescence: a bit of basics and history. In: Papageorgiou, G., Govindjee (Eds.), Chlorophyll a Fluorescence, Advances in Photosynthesis and Respiration, vol. 19. Springer, Netherlands, pp. 1–42.

Kalaji, H.M., Goltsev, V., Bosa, K., Allakhverdiev, S.I., Strasser, R.J., Govindjee, 2012. Experimental in vivo measurements of light emission in plants: a perspective dedicated to David Walker. Photosynth. Res. 114 (2), 69–96.

Krause, G.H., Weis, E., 1991. Chlorophyll fluorescence and photosynthesis: the basics. Ann. Rev. Plant Physiol. Plant Mol. Biol. 42 (1), 313–349.

Ljung, L., 1999. System Identification – Theory for the User. Prentice-Hall, Upper Saddle River, New Jersey.

Ljung, L., 2007. System Identification Toolbox for Use with {MATLAB}.

Moya, I., Cerovic, Z., 2004. Remote sensing of chlorophyll fluorescence: instrumentation and analysis. In: Papageorgiou, G., Govindjee (Eds.), Chlorophyll a Fluorescence, Advances in Photosynthesis and Respiration, vol. 19. Springer, Netherlands, pp. 429–445.

Murchie, E.H., Lawson, T., 2013. Chlorophyll fluorescence analysis: a guide to good practice and understanding some new applications. J. Exp. Botany 64 (13), 3983–3998.

Nedbal, L., 2003. Negative feedback regulation is responsible for the non-linear modulation of photosynthetic activity in plants and cyanobacteria exposed to a dynamic light environment. Biochim. Biophys. Acta (BBA) – Bioenerg. 1607 (1), 5–17.

Nedbal, L., Soukupová, J., Kaftan, D., Whitmarsh, J., Trtílek, M., 2000. Kinetic imaging of chlorophyll fluorescence using modulated light. Photosynth. Res. 66 (1–2), 3–12.

Ounis, A., Evain, S., Flexas, J., Tosti, S., Moya, I., 2001. Adaptation of a PAM-fluorometer for remote sensing of chlorophyll fluorescence. Photosynth. Res. 68 (2), 113–120.

Papageorgiou, G.C., Tsimilli-Michael, M., Stamatakis, K., 2007. The fast and slow kinetics of chlorophyll a fluorescence induction in plants, algae and cyanobacteria: a viewpoint. Photosynth. Res. 94 (2–3), 275–290.

Porcar-Castell, A., Tyystjärvi, E., Atherton, J., Van Der Tol, C., Flexas, J., Pfündel, E.E., Moreno, J., Frankenberg, C., Berry, J.A., 2014. Linking chlorophyll a fluorescence to photosynthesis for remote sensing applications: mechanisms and challenges. J. Exp. Botany 65 (15), 4065–4095.

Schapendonk, A.H.C.M., Pot, C.S., Yin, X., Schreiber, U., 2006. On-line optimization of intensity and configuration of supplementary lighting using fluorescence sensor technology. In: Acta Horticulturae, vol. 711, pp. 423–429.

Schreiber, U., 2004. Pulse-amplitude-modulation (pam) fluorometry and saturation pulse method: an overview. In: Papageorgiou, G., Govindjee (Eds.), Chlorophyll a Fluorescence, Advances in Photosynthesis and Respiration, vol. 19. Springer, Netherlands, pp. 279–319.

Strasser, R.J., Srivastava, A., 1995. Polyphasic chlorophyll a fluorescence transient in plants and cyanobacteria. Photochem. Photobiol. 61 (1), 32–42.

Takayama, K., Nishina, H., Iyoki, S., Arima, S., Hatou, K., Ueka, Y., Miyoshi, Y., 2011. Early detection of drought stress in tomato plants with chlorophyll fluorescence imaging – practical application of the speaking plant approach in a greenhouse. In: IFAC Proceedings Volumes (IFAC-PapersOnline), vol. 18(PART 1), pp. 1785–1790.

van der Tol, C., Verhoef, W., Rosema, A., 2009. A model for chlorophyll fluorescence and photosynthesis at leaf scale. Agric. Forest Meteorol. 149 (1), 96–105.

Walker, D.A., 1992. Concerning oscillations. Photosynth. Res. 34 (3), 387–395.

Walker, D.A., Sivak, M.N., Prinsley, R.T., Cheesbrough, J.K., 1983. Simultaneous measurement of oscillations in oxygen evolution and chlorophyll a fluorescence in leaf pieces. Plant Physiol. 73 (3), 542–549.

Wik, T., Carstensen, A.-M., Pocock, T., 2012. Greenhouse LED lighting control. In: Proceedings of the 17th Nordic Process Control Workshop. Technical University of Denmark, Kgs Lyngby, Denmark, pp. 130–132.

Zhu, X.-G., Wang, Y., Ort, D.R., Long, S.P., 2013. e-Photosynthesis: a comprehensive dynamic mechanistic model of C3 photosynthesis: from light capture to sucrose synthesis. Plant Cell Environ. 36 (9), 1711–1727.